Coexisting patterns of population oscillations: the degenerate Neimark Sacker bifurcation as a generic mechanism

Christian Guill,[1] Benjamin Reichardt,[1] Barbara Drossel,[1] and Wolfram Just[2]

[1] *Institut für Festkörperphysik, TU Darmstadt, Hochschulstrasse 6, 64289 Darmstadt, Germany*
[2] *School of Mathematical Sciences, Queen Mary University of London, Mile End Road, London E14NS, UK*

(Dated: March 1, 2011)

We investigate a population dynamics model that exhibits a Neimark Sacker bifurcation with a period that is naturally close to 4. Beyond the bifurcation, the period becomes soon locked at 4 due to a strong resonance, and a second attractor of period 2 emerges, which coexists with the first attractor over a considerable parameter range. A linear stability analysis and a numerical investigation of the second attractor reveal that the bifurcations producing the second attractor occur naturally in this type of system.

PACS numbers: 87.23.Cc ,05.45.-a

I. INTRODUCTION

The population dynamics of biological species that produce offspring once in their lifetime (semelparous species) provides a generic system that can display a Neimark Sacker bifurcation. A remarkable example is the Pacific sockeye salmon (*Oncorhynchus nerka*), which returns from the ocean to spawn in its native lake and dies afterwards. The sockeye fry spend one season in the lake, feeding on zooplankton and being eaten by predator fish such as rainbow trout, and then migrate to the ocean, from where they return to spawn at the age of 3, 4, or 5 years, with the majority of females reaching an age of 4 years. Several natural sockeye populations display large-amplitude oscillations with a period of 4, which corresponds to the dominant generation time of these fish (an example is given in Figure 1a), a phenomenon generally referred to as cyclic dominance [1]. In contrast to conventional predator-prey systems, the dynamics of the sockeye-trout system in the lake is piecewise continuous in time, due to the salmon migrating to the ocean and returning at the age of 4 (± 1) years. This mechanism, which puts the model in the context of delay dynamical systems, will turn out to be the cause of the interesting dynamical behaviour found in this system. A second important feature of the system is the external periodic drive caused by the yearly rhythm of seasons. The ratio of these two time scales is thus fixed by an internal mechanism which turns out to be vital for the observed phenomena.

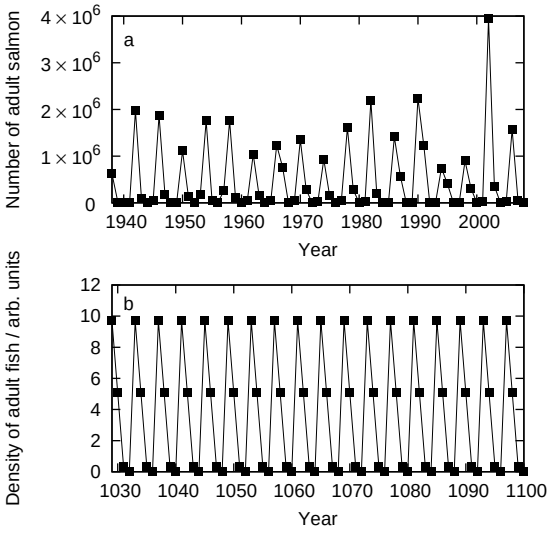

FIG. 1. (a) Empirical time series of the number of adult salmon returning to their native streams. The data shown are those for the Shuswap Lake stock, one of the largest sockeye salmon breading populations in the basin of the Fraser River (British Columbia, Canada). (b) Time series generated with the phenomenological model, Equations (1)–(5). Parameter values used for this diagram are: $\lambda = 0.85$, $a_{sz} = 10$, $a_{ps} = 2$, $c_s = 1$, $c_p = 0.2$, $d_s = 1.1$, $d_p = 0.3$, $\gamma = 0.2$, $\epsilon_1 = 0$, $\epsilon_2 = 0.1$, $K_0 = 2.5$, $\delta = 8$, and $\delta_0 = 0.1$.

While conventional predator-prey systems typically display a Hopf bifurcation [2], the piecewise continuous sockeye-trout model displays a Neimark Sacker bifurcation [3], which is an oscillatory instability in externally driven systems. Since the dominant life span of the salmon is 4 years, the period of the oscillation is naturally close to 4 at the bifurcation, and when the control parameter is further increased beyond the bifurcation, the period becomes locked exactly at 4 due to the strong resonance familiar from the theory of the Neimark Sacker bifurcation [4].

Resonances and the associated synchronisation phenomena are common features in driven systems, with widespread applications in science and technology (cf. [5] for a recent review). But unlike strong resonances one normally requires a fine tuning of parameters, the subtle synchronisation phenomena like phase locking or universal scaling behaviour commonly related with the quasiperiodic transition to chaos [6, 7] may be sensitive to perturbations. In contrast, strong resonances in Neimark Sacker bifurcations generate very stable periodic motion over large regions in parameter space, and thus can provide a vital mechanism for cyclic dominance in biological systems where noise and parameter fluctuations are prevalent.

In this paper, we will explore further the model for the population dynamics of the Pacific sockeye salmon that was introduced in [3]. While the focus of that paper was on reproducing a remarkable feature of a specific biological system, we now investigate more generally the properties of dynamical systems of this type. We will show that the system can display a second attractor, which has the period 2 and coexists with the attractor of period 4. Due to the

strong resonance, the second attractor is clearly visible in bifurcation diagrams where only one of the 6 dimensions of the system is plotted as function of a control parameter. By using computer simulations, we will show that the second attractor arises through a flip bifurcation followed by a subcritical Neimark Sacker bifurcation, and by using a theory that is linearised around the fixed point as well as around the attractor of period 4, we will show that the flip bifurcation can naturally occur soon after the first Neimark Sacker bifurcation.

II. THE MODEL

The dynamics of the biomass of sockeye fry $s_n(t)$, of their predator $p_n(t)$, and of their zooplankton food $z_n(t)$ in year number n during the growth season from spring ($t = 0$) to fall ($t = T$) are given by the following set of coupled differential equations [3]:

$$\begin{aligned}
\frac{d}{dt}s_n(t) &= \lambda g_{sz}(s_n(t), z_n(t)) - g_{ps}(p_n(t), s_n(t)) - d_s \cdot s_n(t) \\
\frac{d}{dt}z_n(t) &= z_n(t) \cdot \left(1 - \frac{z_n(t)}{K_n}\right) - g_{sz}(s_n(t), z_n(t)) \\
\frac{d}{dt}p_n(t) &= \lambda g_{ps}(p_n(t), s_n(t)) - d_p \cdot p_n(t)
\end{aligned} \tag{1}$$

The terms in these equations represent the biomass changes due to eating (with food assimilation efficiency λ) and being eaten, and the losses due to respiration and death. Growth of the zooplankton resource is described by a logistic function with carrying capacity (maximal zooplankton density) K_n, which may change from year to year. The two feeding terms are given by

$$\begin{aligned}
g_{sz}(s, z) &= a_{sz}\frac{z \cdot s}{1 + c_s \cdot s + z} \\
g_{ps}(p, s) &= a_{ps}\frac{s \cdot p}{1 + c_p \cdot p + s}
\end{aligned} \tag{2}$$

These functional forms include saturation at high prey densities, and a predator interference term with interference strengths c_s and c_p for the salmons and their predators, respectively, in the denominator (Beddington functional response [8, 9]). The parameters a_{sz} and a_{ps} are the maximal food ingestion rates of the two consumer species. Like the mortality and respiration rates d_s and d_p, they are related to the rate of the metabolism per unit mass. Therefore, they are smaller for the larger predators [10].

These equations of motion determining the time evolution of the biomass during a single season are supplemented with matching conditions used to determine the biomasses of the species at the beginning of the next season from their values at the end of the previous season(s). To keep the model as simple as possible we assume that no major change in the population of predators occurs. The zooplankton level at the end of one year has no effect on the following year [11], but its saturation value in the next season, K_{n+1}, shows a dependence on the nutrient input due to the number of spawning adults, and thereby on $s_{n+1}(0)$ [12, 13].

$$z_{n+1}(0) = K_{n+1} = K_0 + \left(\delta\frac{s_{n+1}(0)}{\delta_0 + s_{n+1}(0)}\right) \tag{3}$$

$$p_{n+1}(0) = p_n(T) \tag{4}$$

Most importantly the matching condition for the sockeye fry population contains the proportion ϵ_1 and ϵ_2 of surviving sockeye that return to their native lakes at the age of 3 and 5 to spawn and die:

$$s_{n+1}(0) = \gamma[(1 - \epsilon_1 - \epsilon_2)s_{n-3}(T) + \epsilon_1 s_{n-2}(T) + \epsilon_2 s_{n-4}(T)] \tag{5}$$

The proportionality constant γ summarizes survival from juvenile to adult fish in the ocean (including losses to fisheries), spawning success, and egg-to-fry survival. The various factors can be estimated from empirical data [14–16], here we use $\gamma = 0.2$. The fractions of adult sockeyes that return at the age of 3 years (ϵ_1) or 5 years (ϵ_2) instead of 4 years is measured in the real populations. In the populations where cyclic dominance is observed, typically close to 10% of the fish spawn at the age of 5 years, while those returning at the age of 3 years are mainly small-sized males that do not affect the number of fertilized eggs [1]. We therefore neglect the latter in the numerical simulations presented here.

On the one hand the model may be considered as a very simple example of a piecewise smooth dynamical system [17], where the discontinuities are contained in the matching condition between seasons. On the other hand the

model may be considered as a periodically driven non autonomous system where the external drive is provided by the seasons. It is therefore an obvious approach to consider the stroboscopic map. If we denote by $\Phi_{[0,T]}$ the flow of the differential equation (1) the biomasses at the beginning and at the end of the year $n+1$ are related by

$$(s_{n+1}(T), p_{n+1}(T), z_{n+1}(T)) = \Phi_{[0,T]}(s_{n+1}(0), p_{n+1}(0), z_{n+1}(0)) \tag{6}$$

The condition (3) tells us that the zooplankton is entirely determined by sockeye population so that z_n drops from Eq.(6) as a dynamical variable. Taking Eqs.(4) and (5) into account the remaining biomass evolution can be written as

$$\begin{aligned} s_{n+1}(T) &= h_s(\epsilon_1 s_{n-2}(T) + (1-\epsilon_1-\epsilon_2)s_{n-3}(T) + \epsilon_2 s_{n-4}(T), p_n(T)) \\ p_{n+1}(T) &= h_p(\epsilon_1 s_{n-2}(T) + (1-\epsilon_1-\epsilon_2)s_{n-3}(T) + \epsilon_2 s_{n-4}(T), p_n(T))\,. \end{aligned} \tag{7}$$

Thus we arrive at a six dimensional time discrete dynamical system. The computation of the right hand sides, h_s and h_p, requires the integration of the equations of motion, Eq.(1), a task which can be accomplished easily by numerical means. However, the structure of the map (7), induced by the matching condition (5) will turn out to be crucial for the properties of the population dynamics.

III. THE MAIN BIFURCATION GENERATING CYCLIC DOMINANCE

It is our main purpose to pinpoint an underlying generic mechanism which creates stable cyclic motion among the populations in our model. For that purpose we employ a brief bifurcation analysis for realistic combinations of the parameters of the model. Given the fairly large number of parameters in our model and the fairly large number of degrees of freedom we just resort to plain numerical simulations. In fact, employing for our specific purpose numerical continuation tools like matcont [18] our auto [19] would be using a sledge-hammer to crack a nut. In addition, our specific numerical study mimics approaches which could be used in evaluating empirical data, and thus could be a guide for their analysis.

Figure 2 shows the bifurcation diagram for a realistic set of parameter values. For each value of the parameter δ, several initial conditions were drawn at random from uniform probability distributions on a 6-dimensional cube $(0; 10]$. When coexisting attractors were found, these were numerically continued until they became unstable. After a transient time of 5000 years (longer close to bifurcations), the values for $s_n(T)$ were plotted for 20 additional years. As δ increases, the fixed point becomes unstable due to a Neimark Sacker bifurcation, and a quasiperiodic attractor arises. At $\delta \simeq 4.47$, trajectories can become locked exactly at the period 4, but the quasiperiodic attractor remains stable until $\delta \simeq 4.6$. This picture is consistent with a Neimark Sacker bifurcation close to a strong resonance of order 1:4, which is known to display quite a subtle bifurcation structure [4], including the creation of homoclinic tangles.

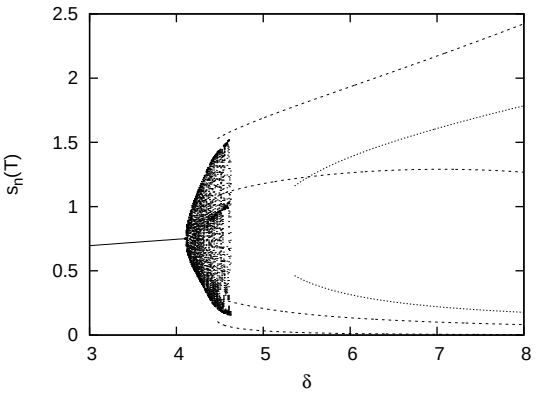

FIG. 2. Bifurcation diagram of the biomass of the sockeye fry at the end of their first year. Parameter values used for this diagram are as in figure 1.

At $\delta \simeq 5.36$, a second attractor with period 2 appears. Such a feature is normally not related with the generic strong resonant Neimark Sacker bifurcation mentioned above. The two arms of this attractor appear as if they are created as an unstable period two orbit at $\delta \simeq 5.1$ via a flip bifurcation from the already unstable fixed point. The unstable arms then become stable at $\delta \simeq 5.36$ when the complex conjugate pair of eigenvalues moved back into the

unit circle. Even without continuation tools tracking saddle orbits we are able to vindicate this picture by evaluating the size of the basin of attraction of the period two attractor and by monitoring the transient dynamics.

Figure 3 shows an example of the transient dynamics in the stable period two regime. Since only every other iteration is displayed the transient consists of a damped oscillation with a period close to 4. By measuring the decay rate τ of the oscillations around the stable period two orbit for different values of δ we determined the bifurcation value δ_c with an accuracy of 10^{-6}. Sufficiently close to the bifurcation, τ goes linearly to 0 as the instability is approached (lower inset in Figure 3). We then estimated the diameter of the basin of attraction by using a one dimensional cross section along the direction of the first salmon population. Initial conditions were distributed along this cross section, and those trajectories which return to the period two state determine the extent of the basin along this direction in phase space. Figure 4 shows the result for the size of the basin, and the characteristic square root law with regard to the distance from the bifurcation point is recorded. Thus the bifurcation which causes the stability of the period two state is clearly a subcritical bifurcation.

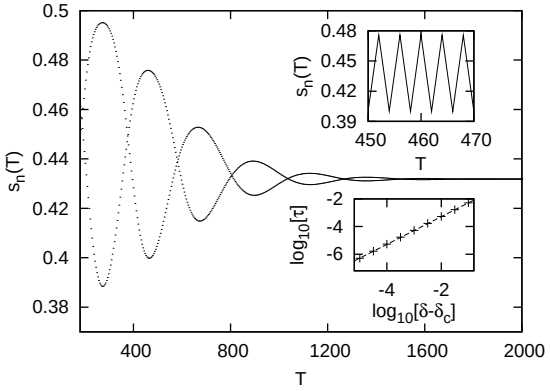

FIG. 3. Trajectory approaching the period 2 attractor. $\delta = 5.45$, all other parameters are as in figure 1. Only every second data point is plotted. Upper inset: close-up of the trajectory. Lower inset: decay rate of the oscillations when approaching the instability. The dashed line is a linear function fitted to the numerically determined decay rates, yielding $\delta_c = 5.356111 \pm 5 \cdot 10^{-7}$.

All these results demonstrate that the second attractor emerges due to a subcritical Neimark Sacker bifurcation, and this secondary Neimark Sacker bifurcation is intimately related to the bifurcation creating the stable period four attractor. We are now going to uncover the underlying mechanism by analytical considerations.

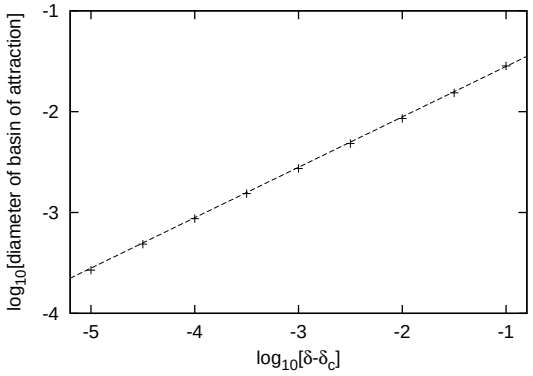

FIG. 4. Size of the basin of attraction of the period 2 attractor. Parameters are as in figure 2, and $\delta_c = 5.356111$. The dashed line is a power law with exponent 1/2.

IV. LINEAR STABILITY ANALYSIS

A linear stability analysis of the dynamical system close to the first Neimark Sacker bifurcation reveals that the scenario outlined in the previous section is indeed a natural scenario for this type of system. The continuous population dynamics during the season, together with the matching conditions applied between two seasons, can be viewed as a Poincaré map, Eq.(7), giving the sockeye and predator biomasses at the end of one year as function of the biomasses at the end of the previous years. Close to the fixed point (s^*, p^*), the dynamics can be approximated by linear terms. Denoting the distance of the biomasses from their fixed point value by $\delta s_n = s_n(T) - s^*$ and $\delta p_n = p_n(T) - p^*$, the linear approximation of Eq.(7) has the form

$$\begin{pmatrix} \delta s_{n+1} \\ \delta s_n \\ \delta s_{n-1} \\ \delta s_{n-2} \\ \delta s_{n-3} \\ \delta p_{n+1} \end{pmatrix} = \begin{pmatrix} 0 & 0 & \alpha\epsilon_1 & \alpha(1-\epsilon_1-\epsilon_2) & \alpha\epsilon_2 & \beta \\ 1 & 0 & 0 & 0 & 0 & 0 \\ 0 & 1 & 0 & 0 & 0 & 0 \\ 0 & 0 & 1 & 0 & 0 & 0 \\ 0 & 0 & 0 & 1 & 0 & 0 \\ 0 & 0 & \bar{\alpha}\epsilon_1 & \bar{\alpha}(1-\epsilon_1-\epsilon_2) & \bar{\alpha}\epsilon_2 & \bar{\beta} \end{pmatrix} \begin{pmatrix} \delta s_n \\ \delta s_{n-1} \\ \delta s_{n-2} \\ \delta s_{n-3} \\ \delta s_{n-4} \\ \delta p_n \end{pmatrix} \tag{8}$$

where

$$\begin{aligned} \alpha &= \frac{\partial h_s(s^*,p^*)}{\partial s^*}, \quad \beta = \frac{\partial h_s(s^*,p^*)}{\partial p^*} \\ \bar{\alpha} &= \frac{\partial h_p(s^*,p^*)}{\partial s^*}, \quad \bar{\beta} = \frac{\partial h_p(s^*,p^*)}{\partial p^*} \end{aligned} \tag{9}$$

denote the partial derivatives of the Poincar?? map at the fixed point. These parameter values can in principle be obtained by a numerical evaluation of the population dynamics, Eq.(1), close to the fixed point. Any consistent underlying dynamical model should give a negative value of the parameter β, since an increase in trout biomass leads to a decrease in salmon biomass. The other parameters in Eq.(9) have to be non-negative, since more parents imply more offspring and since an increase in salmon biomass leads to an increase in trout biomass. However, it is notoriously difficult to derive such conditions from equations of motion like Eq.(1).

The eigenvalues of the matrix in Eq.(8) determine the nature of the dynamics near the bifurcation. When all eigenvalues have an absolute value smaller than 1, the fixed point is stable, and the dynamics converges to this fixed point. When the absolute value of one or more eigenvalues is larger than 1, the fixed point is unstable, and the dynamics approaches a different attractor. The eigenvalues μ satisfy the characteristic equation

$$\mu^5(\bar{\beta}-\mu) + [\epsilon_1\mu^2 + (1-\epsilon_1-\epsilon_2)\mu + \epsilon_2][\beta\bar{\alpha} - \alpha(\bar{\beta}-\mu)] = 0\,. \tag{10}$$

In order to understand the possible bifurcation scenarios, we first consider the case that only the parameters α, β and $\bar{\beta}$ are nonzero. This means that the four salmon lines are independent from each other, $\epsilon_1 = \epsilon_2 = 0$, and from the trout, $\bar{\alpha} = 0$. The eigenvalues of the matrix are $\bar{\beta}$, 0, and the four fourth roots of α. The eigenvalue $\bar{\beta}$ characterises the time evolution of the trout, which is decoupled from the salmon in the considered case. Global stability criteria require this eigenvalue to be smaller than one, $0 \le \bar{\beta} < 1$. The eigenvalue 0 is due to the fifth column of the matrix being redundant if $\epsilon_2 = 0$. The four fourth roots of α describe the salmon dynamics in the vicinity of the fixed point. The sequence δs_n has trivially the period 4 and simply iterates the initial four values, with an amplitude decreasing for $\alpha < 1$ and increasing otherwise. When α is increased from a value smaller than 1 to a value larger than 1, all four eigenvalues $\alpha^{1/4}$ cross the unit circle simultaneously, and the fixed point becomes unstable. This degeneracy is lifted when the other parameters, ϵ_1, ϵ_2, and $\bar{\alpha}$, are made nonzero. As long as these parameters are not large, one can expect the four main eigenvalues to remain close to the unit circle, implying a (possibly damped) oscillation with a period close to 4. If the complex conjugate pair of eigenvalues is the first one to cross the unit circle, a Neimark Sacker bifurcation occurs. If the negative eigenvalues crosses the unit circle first, a flip bifurcation occurs. For the parameter values chosen in the simulation (Figure 2), the Neimark Sacker bifurcation is observed first.

The entire bifurcation scenario can be computed from Eq.(10) using the Schur-Cohn-Jury criterion [20], but the main mechanism which is at the heart of the bifurcation discussed in the previous section can be already uncovered if we resort to a perturbative approach. In order to gain some analytical insights, we assume that the parameters ϵ_1, ϵ_2, and $\bar{\alpha}$ are so small that the change in μ can be calculated approximately by performing a first order Taylor expansion in $\alpha - 1$, close to the bifurcation. By implicit differentiation of Eq.(10) we obtain for the relative change of

the eigenvalues close to the unit circle

$$\frac{\delta\mu}{\mu_0} = \frac{\alpha-1}{4} - \begin{cases} \dfrac{(-\beta)\bar{\alpha}}{4(1-\bar{\beta})} & \text{if} \quad \mu_0 = 1 \\ \dfrac{\epsilon_1+\epsilon_2}{2} - \dfrac{(-\beta)\bar{\alpha}}{4(1+\bar{\beta})} & \text{if} \quad \mu_0 = -1 \\ \dfrac{\epsilon_1+\epsilon_2}{4} - \dfrac{(-\beta)\bar{\alpha}\bar{\beta}}{4(1+\bar{\beta}^2)} \mp \dfrac{i}{4}\left(\epsilon_1 - \epsilon_2 + \dfrac{(-\beta)\bar{\alpha}}{4(1+\bar{\beta}^2)}\right) & \text{if} \quad \mu_0 = \pm i \end{cases} \tag{11}$$

where μ_0 denotes the eigenvalue of the unperturbed case. The real part of this ratio $\delta\mu/\mu_0$ determines the stability properties of the eigenmode. As long as the parameter $\bar{\beta}$ is not too small, i.e. as long as the decay of the trout population is not massive, the negative contribution to the positive real eigenvalue (the case $\mu_0 = 1$) dominates, and this mode remains stable on changing the bifurcation parameter $\alpha - 1$. Thus no saddle node bifurcation is expected to occur. The order of the other two cases, a bifurcation caused by a negative eigenvalue (the case $\mu_0 = -1$) and a strongly resonant Neimark Sacker bifurcation (the case $\mu_0 = \pm i$) is now determined by the balance between the unfolding parameters. If $\epsilon_1 + \epsilon_2$ is sufficiently large compared to $\bar{\alpha}$, the Neimark Sacker bifurcation appears first, as the negative contribution to the second case in Eq.(11) is larger (in modulus) than the negative contribution to the third case. In quantitative terms Eq.(11) yields for the suppression of the saddle node bifurcation the inequality

$$\frac{(-\beta)\bar{\alpha}}{1-\bar{\beta}^2} > \epsilon_1 + \epsilon_2 \tag{12}$$

whereas the Neimark Sacker bifurcation precedes the flip bifurcation if

$$\epsilon_1 + \epsilon_2 > \frac{(-\beta)\bar{\alpha}(1-\bar{\beta})}{(1+\bar{\beta})(1+\bar{\beta}^2)} \tag{13}$$

is satisfied (remember that $\beta < 0$ and $0 < \bar{\beta} < 1$).

These considerations show that as long as the coupling between the different salmon lines and between the salmon and the trout is small compared to the coupling between salmon parents and offspring (i.e. $\epsilon_1 \ll 1$, $\epsilon_2 \ll 1$, and $\bar{\alpha} \ll 1$), the oscillation period of the population is close to four. If the coupling between the salmon lines is finite and beyond a threshold value determined by the small coupling between the salmon and the trout (i.e. by the parameter $\bar{\alpha}$, cf. Eq.(13)) the period four oscillating mode becomes unstable first as the bifurcation parameter α is increased, and the complex conjugate eigenvalues close to the imaginary axis are pushed towards the unit circle. The complex conjugate eigenvalues are therefore the first ones to cross the unit circle followed by the eigenvalue on the negative real axis. But we require as well a decay rate for trouts which is not excessively large, Eq.(12), to prevent the saddle node bifurcation to occur. In fact, in the limit $\bar{\beta} \to 0$ the two conditions, Eqs.(12) and (13) become mutually exclusive. Thus the dynamics of the predators play an important role and the scenario would not appear if an adiabatic elimination of the trout population would have been an option. The scenario found in the computer simulations, where first a Neimark Sacker bifurcation occurs and then a flip bifurcation, is thus a generic scenario in this type of system. Clearly, our linear analysis cannot keep track of the stability properties of the period two orbit created in the secondary flip bifurcation. Certainly this orbit inherits its stability properties from the bifurcating fixed point, but we cannot predict without a tedious normal form calculation whether the two unstable complex conjugated eigenvalues move back into the unit circle, although such a re-entrance phenomenon is not uncommon. While we observed the subcritical Neimark Sacker bifurcation on the period-2 orbit for a broad set of parameter values, it did not occur in other regions of parameter space. But the presented analytical considerations have shown that the stable period two and period four oscillations are caused by the same degenerate Neimark Sacker bifurcation, and we were able as well to derive criteria for the occurrence of this scenario.

Since the parameters ϵ_1 and ϵ_2, that determine the age composition of the spawning salmon, are important determinants of the order of the bifurcations, we also tested numerically the ranges of these parameters that give rise to the initial Neimark-Sacker bifurcation and the strong resonance in the phenomenological model, Equations (1)–(5). When 3 year old salmons can be neglected ($\epsilon_1 = 0$), the strong resonance appears if $\epsilon_2 \lesssim 0.4$. For $\epsilon_1 = 0.1$, the strong resonance is seen for $\epsilon_2 \lesssim 0.35$. If the fraction of 4 year old salmon (s_{n-3}) in Equation (5) is not dominant, only quasiperiodic oscillations are observed. If the population is dominated by salmons returning at the age of 3 (e.g. $\epsilon_1 = 0.9$ and $\epsilon_2 = 0$), a strong resonance of order 1:3 appears.

V. CONCLUSIONS

We have shown that a three-species population dynamics model can serve as a model system for observing the coexistence of two attractors, one of period four and one of period two. This is remarkable, since this type of

scenario is of codimension 3, requiring a Neimark-Sacker bifurcation occurring with a period close to four, and a third eigenvalue crossing the unit cycle for a nearby value of the control parameter. We have identified conditions such that the bifurcation of high codimension does not require fine tuning of additional parameters. First of all, the external stimulus of yearly season and the return of species for spawning provides the strong resonance condition of the Neimark Sacker bifurcation and the reduction to a time discrete dynamical model. The second important ingredient is a predator population which actively takes part in the dynamics and cannot be taken into account on a plain adiabatic description. Finally a weak coupling between the different spawning populations is required. While the zooplankton provides the source for keeping the nonequilibrium dynamics going, it does not independently take part in the dynamics but depends solely on the current salmon population. While our considerations have been based on a simple, phenomenological model, Eq.(1), we should emphasise that the conclusions have a fairly broad remit as the time discrete dynamics (7) only takes a few generic features of the model into account. Population models that have discrete generations can thus represent a natural situation for a scenario that was previously expected to require very improbable special conditions.

At a more fundamental abstract level the model proposed in this contribution is at the interface between piecewise smooth dynamical systems and driven delay dynamics, both being fields of active research in applied dynamical systems theory [17, 21]. Although being a standard aspect of bifurcation theory, the mechanism presented here could have a wider impact for the study of robust periodic motion and synchronisation in a large class of experimentally relevant setups in science and engineering.

[1] W. E. Ricker, Can. J. Fish. Aquat. Sci. **54**, 950 (1997).
[2] M. L. Rosenzweig, Science **171** 385 (1971).
[3] C. Guill, B. Drossel, W. Just, and E. Carmack (submitted), arXiv:1006.2923.
[4] Y. A. Kuznetsov, Elements of Applied Bifurcation Theory (Springer-Verlag, New York, 2004).
[5] A. Pikovsky, M. Rosenblum, and J. Kurths, Synchronization: a universal concept in nonlinear sciences (Cambridge University Press, Cambridge, 2003).
[6] M. J. Feigenbaum, L. P. Kadanoff, and S. J. Shenker, Physica D **5**, 370 (1982).
[7] P. Cvitanovic, G. H. Gunaratne, and M. J. Vinson, Nonlin. **3**, 873 (1990).
[8] J. R. Beddington, J. Anim. Ecol. **44**, 331 (1975).
[9] G. T. Skalski and J. F. Gilliam, Ecology **82**, 3083 (2001).
[10] J. H. Brown, J. F. Gillooly, A. P. Allen, V. M. Savage, and G. B. West, Ecology **85**, 1771 (2004).
[11] D. A. Levy and C. C. Wood, Bull. Math. Biol. **54**, 241 (1992).
[12] S. M. Gende, R. T. Edwards, M. F. Willson, and M. S. Wipfli, BioScience **52**, 917 (2002).
[13] J. Hume, K. Shortreed, and T. Whitehouse, Sockeye fry, smolt, and nursery lake monitoring of Quesnel and Shuswap lakes in 2004. (2005) Available at http://www.unbc.ca/qrrc/historical_research.html
[14] C. J. Walters and M. J. Staley, Can. Spec. Publ. Fish. Aquat. Sci. **96**, 375 (1987).
[15] G. B. Pauley, R. Risher, and G. L. Thomas, Species profiles: life histories and environmental requirements of coastal fishes and invertebrates (Pacific Northwest) – Sockeye salmon. US Dep. Int., Fish and Wildlife Service, Biological Report 82(11.116) (1989).
[16] J. M. B. Hume, K. S. Shortreed, and K. F. Morton, Can. J. Fish. Aquat. Sci. **53**, 719 (1996).
[17] M. di Bernardo, C. J. Budd, A. R. Champneys, and P. Kowalczyk, Piecewise-smooth dynamical systems: Theory and Applications (Springer-Verlag, London, 2008).
[18] http://www.matcont.ugent.be/
[19] http://www.ma.hw.ac.uk/˜gabriel/auto07/auto.html
[20] E. I. Jury, Proc. IRE **50**, 1493 (1962).
[21] W. Just, A. Pelster, M. Schanz, and E. Schöll (Eds.), Phil. Trans. Roy. Soc. A **368**, 301 (2010).